

# Martensitic Transformation and its Effect on the Interfacial Debonding in Single Ni-Ti Fibre/ Epoxy Composite

Yousef Payandeh<sup>1a</sup>, Fodil Meraghni<sup>1</sup>, Etienne Patoor<sup>1</sup>, André Eberhardt<sup>2</sup>

Laboratoire de Physique et Mécanique des Matériaux (LPMM-UMR CNRS 7554)  
1-Arts et Métiers ParisTech, Metz , 4 rue Augustin Fresnel, 57078, Metz, France  
2- ENIM, Ile du Saulcy, 57045, Metz, France

**Abstract.** The effect of martensitic transformation in single Ni-Ti shape memory wire epoxy matrix composite was investigated. The Ni-Ti wire was received in as drawn condition and was subjected to three different heat treatments in order to obtain wires with different transformation characteristics. The in-situ observations of the interfacial debonding and sliding behaviour during the pull-out test were carried out. It is observed that when there is no phase transformation the debonding propagates rapidly whilst it is slow when there is wire phase transformation or martensitic reorientation. It is found that the debonding rate depends on the applied crosshead speed as well as the length change during phase transformation.

## 1. Introduction

Shape Memory Alloys (SMAs) are metallic alloys that can undergo martensitic phase transformations as a result of applied thermomechanical loads and are capable of recovering permanent strains when heated above a certain temperature. The key characteristic of all SMAs is the occurrence of a martensitic phase transformation between the austenitic phase and the different variants of the low temperature, low symmetry martensitic phase [1]. In near equiatomic Ni-Ti alloys, the shape memory effect and superelasticity occur in association with the thermoelastic martensitic transformation from the parent phase ( $\beta$ ) with a B2 structure to the phase with a monoclinic B19' structure, or more often in association with the two-step transformation from the  $\beta$  to a trigonal phase (so called R-phase) and then to the B19' phase [2].

In order to guaranty adequate stiffness and ultimate strength of functional elements, together with high durability and long-term performance, SMAs are sometime embedded into a polymeric matrix [3]. Good adhesion between polymer and Ni-Ti shape memory alloys is a prerequisite for all potential applications of this type of hybrid system [4]. It is well recognized that the mechanical behaviour of many composite materials depends largely on the properties of the fibre/matrix interface [5-8]. One of the fundamental problems in the field of fibre-polymer composites deals with the control of the degree of adhesion between the usually more rigid fibre and the relatively ductile polymer matrix [9]. In fact, when composites are loaded, stress transfer would take place across the fibre/matrix interface. The mechanical properties of the composites depend critically upon the efficiency of the stress transfer during fibre pull-out [5]. A composite system with large interfacial shear strength,  $\tau_i$ , (excellent fibre-matrix bonding) has high strength due to effective stress transfer from the matrix to the fibres [7].

The fibre pull-out test has been well accepted as one of the most important test methods developed as a means of investigating the interfacial adhesion quality and interfacial properties between fibres and matrix and the elastic stress transfer in the fibre pull-out problem [10-14]. The pull-out test has been extensively used for this meaning in a SMA fibre composite as studied in several works [15-19]. In the present work, the debonding

---

<sup>a</sup> email: [Yousef.payandeh@metz.ensam.fr](mailto:Yousef.payandeh@metz.ensam.fr)

propagation in the single Ni-Ti shape memory wire composite samples were investigated in order to verify the effect of martensitic phase transformation on the debonding rate.

## 2. Experimental procedure

The composite material studied in this work is a near equiatomic Ni-Ti shape memory wire epoxy matrix composite. The 1 mm diameter wire was supplied by the Nimesis Company. In order to have the shape memory wire with different transformation characteristics three heat treatment cycles were chosen. The transformation temperatures were identified, using the DSC technique. The results are listed in table 1. The oxide layer was then removed from the wire surface, and then the wire was cleaned and dried. The Ni-Ti wires show the Austenite (B2)  $\rightarrow$  R-phase  $\rightarrow$  Martensite (B19') transformation sequence on cooling and the B19'  $\rightarrow$  B2 on heating.

**Table 1.** The transformation temperatures (K) for different heat treatments

Alloy	Heat treatment	$M_f^{(1)}$	$M_s^{(1)}$	$R_f^{(1)}$	$R_s^{(1)}$	$A_s^{(1)}$	$A_f^{(1)}$
M- 550	823 (K) for 30 min	290	307	307	314	327	350
M- 450	723 (K) for 60 min	252	275	314	325	322	338
M- 400	673 (K) for 60 min	203	265	318	333	320	337

(1)-  $M_s$ ,  $M_f$ ,  $R_s$ ,  $R_f$ ,  $A_s$  and  $A_f$  are the Martensite, R-phase and Austenite start and finish temperatures respectively.

An epoxy -amine mixture (epoxy: D.E.R. 332 supplied by Sigma-Aldrich Chemie GmbH and Amine: Lonzacure Detda 80 supplied by Lonza Ltd.) was cast into a preheated metallic mould in which a single Ni-Ti wire was located in the centre of each hole. The composite was then cured at 413 K for 1 h, post-cured for 5 h at 438 K and cooled to room temperature.

The composite sample is a cylinder with diameter of 15 mm and about 50 mm in length. The embedded wire length,  $L$ , is about 50 mm which corresponded to a wire aspect ratio of  $L/2a \approx 50$ . The nominal wire volume fraction equals to 0.44 %.

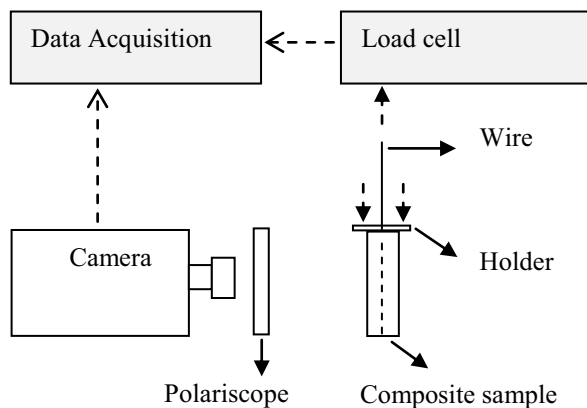


**Fig. 1.** Experimental set-up

The composite specimen was put under a metallic holder, which had a 3 mm diameter hole at the centre. The centre of the wire was placed at the centre of the hole in order to allow the wire to be pulled out freely from the specimen. The pull-out test was conducted in air at the temperature about 293 K by fixing the metallic piece and applying a tensile load to the free end of the wire at a constant displacement rate of 0.5 mm/min ( $V_i$ ). For comparison, some specimens were tested with the displacement rate of 0.1 mm/min. The experimental set-up is shown in Fig. 1. The in-situ observations of the interface debonding and sliding behaviour during the pull-out test were carried out using a digital camera which was located in back of polariscope. Several photos were taken during the experiment.

### 3. Results and discussion

The mechanical behaviour of the wires is shown in Fig. 2 and 3. The M-550 wires at the test temperature are martensitic which was formed in self-accommodating manner. In the M-400 and M-450 wires, the stable phase is R-phase at the test temperature. Thus, by applying the external stress, the martensitic reorientation occurs in M-550 whilst in M-450 and M-400, at first the reorientation of the R-phase occurs (first plateau) and then the martensitic transformation takes place (second plateau).

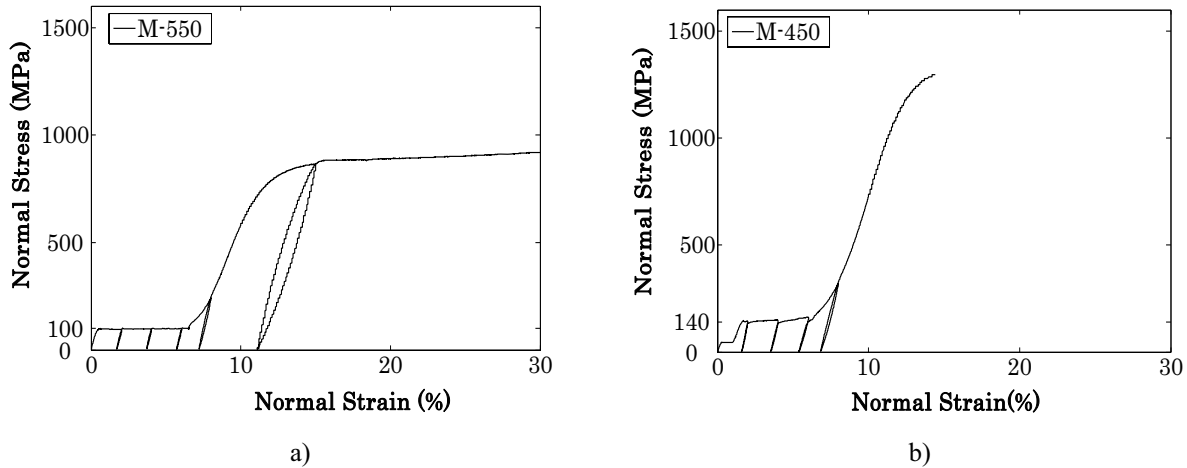


Fig. 2. Stress -Strain diagram for a) M-550 and b) M-450 wires

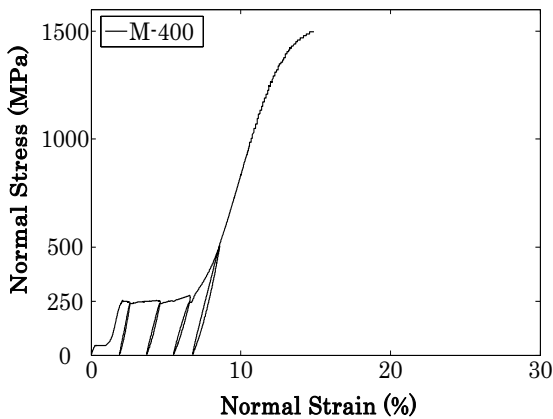


Fig. 3. Stress -Strain diagram for M-400 wire

The stress at which the martensite reorients in the M-550 wires is about 100 MPa ( $F \approx 80$  N) at room temperature. In the case of M-450 wires the martensitic transformation occurs under a stress about 140 MPa ( $F \approx 110$  N). The M-400 wires transform to martensite under a stress about 250 MPa ( $F \approx 200$  N) at the same temperature. In what follows, these stresses/loads will be denoted by transformation stresses/loads.

The results of pull-out test are shown in the Fig. 4 and 5. The onset of debonding is indicated in each figure. The load at which the debonding begins is denoted by debonding load. Fig. 4 illustrates that in both samples with M550 and M450 wires the martensitic reorientation/ transformation of the free part of wires occurs before that debonding begins. In M400 wire specimens the martensitic transformation does not occur before debonding's onset (Fig. 5). In the other word, the transformation load in M550 and M450 wires is less than debonding load whilst in M-400 wire the debonding load is less than transformation one.

It is worth noting that in M-550 and M-450 samples, during debonding propagation the load remains constant (Fig. 4) while it increases during propagation of debonding in the specimens with M-400 wires. As it shown in Fig. 5-b, the load remains constant as soon as it becomes more than the transformation load ( $\approx 200$  N) which is discussed later.

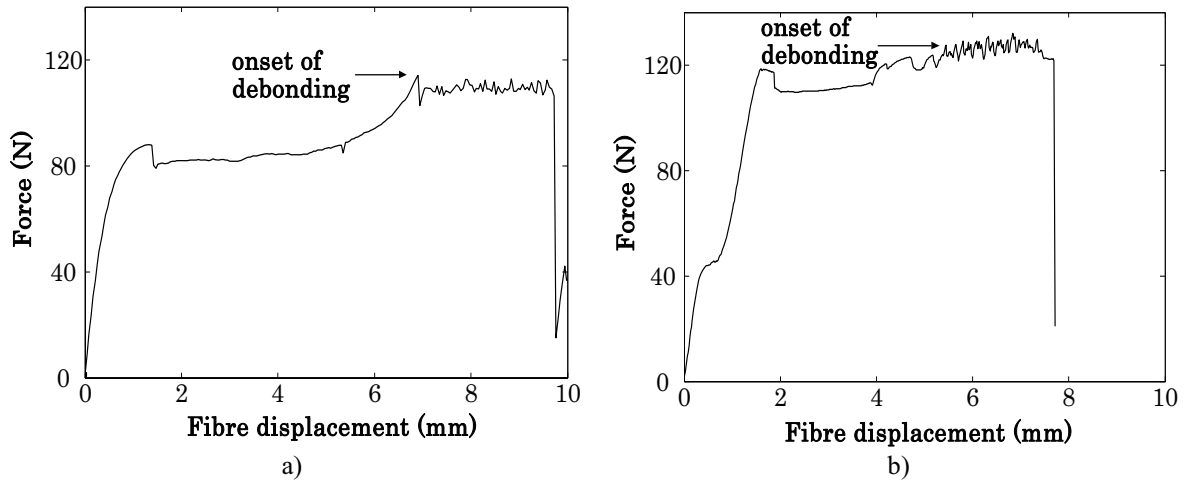


Fig. 4. Force - Displacement diagram for the specimens with (a) M-550 and (b) M450 wire

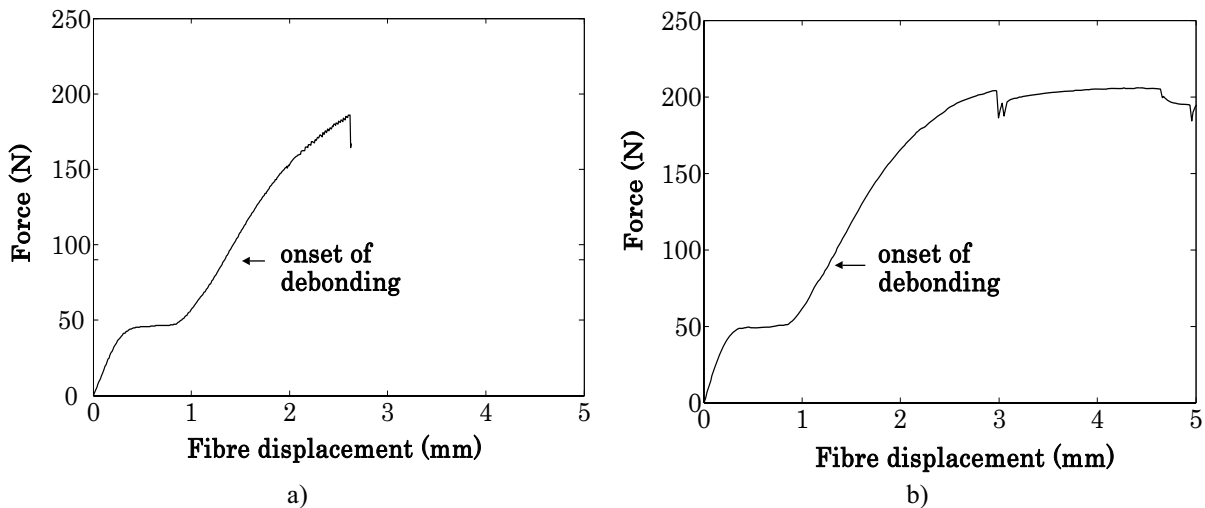


Fig. 5. Force - Displacement diagram for the specimens with M-400 wire (a) without and (b) with transformation

Fig. 6-a shows the debonding rate versus time of debonding for the specimens with M-550 wires. From this figure, apart from the last step, the debonding rate is constant and is about 8.5 mm/min. In the last part (critical length) the debonding propagates with the rate of 14.1 mm/min. The mean value is equal to 9.2 mm/min. The average debonding rate for the other M550 samples varies between 8.3 and 9.3. The debonding rate for a sample with M-400 wire is shown in Fig. 6-b. As it shown, the debonding propagates in this specimen with the rate from 13.5 to 18.3, and 23.5 mm/min for the last part. The average debonding rate for the M400 samples varies between 14.4 and 17.3 mm/min. In the M-400 samples with second plateau (e.g. Fig. 5-b), the average debonding rates are close to the lower value (14.4) and the average debonding rates which are close to the upper one (17.3) correspond to the M-400 samples without second plateau (e.g. Fig. 5-a). In the case of M450 wire composite samples, the debonding propagates with an average rate which varies between 10.6 and 11.3 for different specimens. The discrepancy in debonding rates for three types of samples is associated with martensitic reorientation/ transformation which take place in the M-550/ M450 wires during loading. In other word, because of increasing the length during martensitic reorientation/ transformation in M-550/ M450 wires, the debonding rate in these specimens is small in comparison to the samples with M-400 wires. In some specimens with M-400 wire, the phase transformation occurs before that the interface is debonded entirely (Fig. 5-b). Fig. 6-c shows the debonding rate versus time for this specimen. As it shown in Fig. 6-c, the interface debonds with the rate of about 15 mm/min and after about 150 seconds the rate decreases to 10.8 and 10.9 mm/min. This phenomenon was repeated in some other samples (with M-400 wire) and can not be attributed for experimental errors. In these specimens, the embedded length is a little more than the embedded length in the other samples with M-400 wires, thus the debonding duration is a little more than the others. In the last few seconds, the load becomes more than transformation load ( $\approx 200$  N) and the phase transformation begins just before that the interface debonds completely. As a result, the debonding rate decreases (Fig. 5-b and 6-c).

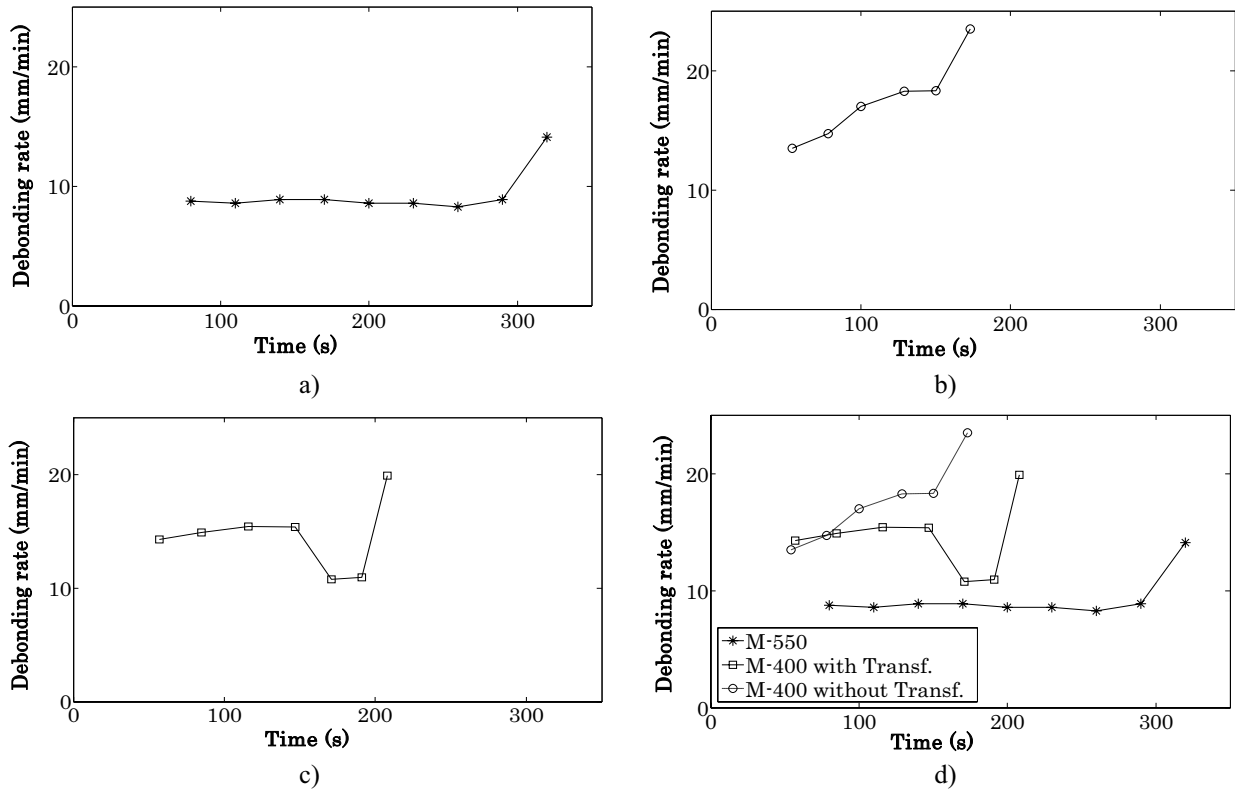


Fig. 6. Debonding rate for a specimen with a) M-550, b) M-400 and c) M-400 wires d) a, b and c for comparison

Therefore, it can be claimed that the length changes during martensitic reorientation in M-550 or martensitic transformation in M-450 or sometimes in M-400, is the sole reason of decreasing in debonding rate. In the specimens with M-400, because there is no phase transformation, the interface debonds rapidly.

Table 2. Debonding rate,  $v_d$ , displacement rate  $V_i$  (mm/min) and  $\varepsilon^{tr}$  and their relationship

Sample	Deformation mode	$\varepsilon^{tr}$ (average) <sup>(1)</sup>	$v_d$ (mm/min)	$v_d$ (average) <sup>(1)</sup> (mm/min)	$\varepsilon^{tr} \cdot v_d$	$V_i$
M550	M. Reorientation	0.056	8.3-9.3	8.84	0.495	0.5
M450	M. Transformation	0.045	10.6-11.3	10.95	0.493	0.5
M400 with MT	M. Transformation	0.044	10.8-11.4	11.25	0.495	0.5
M400 without MT	-	-	15.7-17.3	16.58	-	0.5
M550	M. Reorientation	0.056	1.9- 1.98	1.95	0.109	0.1

(1)- The average  $\varepsilon^{tr}$  and  $v_d$  were calculated using several samples.

It should be noticed that when an embedded stress free SMA wire is subjected to the tensile load during pull-out test, the wire phase transformation/reorientation can not occur before interfacial debonding, because the phase transformation/reorientation is accompanied by a large inelastic strain. But the transformation occurs immediately after partial debonding; and the length change during phase transformation causes the load to remain constant while debonding propagates (Fig. 4-a, 4-b and 5-b). It also causes the rate of debonding to decrease because the test is carried out in the constant displacement rate. The following equation was proposed to relate the displacement rate ( $V_i$ ) to the debonding rate ( $v_d$ ) and transformation strain ( $\varepsilon^{tr}$ ) [20].

$$V_i = v_d \cdot \varepsilon^{tr}$$

The debonding rate,  $v_d$ , and transformation strain,  $\varepsilon^{tr}$ , for each type of specimen has been measured from experimental data and the results are shown in Table 2. The equation 1 can be validated by comparing the last two columns.

## 4. Conclusion

The effect of martensitic transformation on the debonding propagation in single Ni-Ti shape memory wire composite was investigated. It was experimentally found that:

In both samples with M550 and M450 wires the martensitic reorientation/ transformation of the free part of wires occurs before that debonding begins. In M400 wire specimens, the martensitic transformation does not occur before debonding's onset.

The average debonding rate for the M550 samples varies between 8.3 and 9.3 mm/min for different specimens. In the case of M450 wire composite samples, the debonding propagates with an average rate that varies between 10.6 and 11.3 mm/min for different specimens. The debonding rate for a sample with M-400 wire is different and varies between 14.4 and 17.3 mm/min.

In both samples with M550 and M450 wires the debonding propagates with a constant rate.

It can be claimed that the length changes during martensitic reorientation in M-550 or martensitic transformation in M-450 or sometimes in M-400, is the sole reason of decreasing in debonding rate. In the specimens with M-400, because there is no phase transformation, the interface debonds fast.

The debonding rate depends on the displacement rate as well as the transformation strain. The equation  $v_d = V_i / \epsilon^{\text{tr}}$  was proposed to relate these three parameters.

**Acknowledgements** The authors would like to acknowledge Nimesis Technology Company, L. Peltier and S. Boulard, A. Nachit and M. Wary for their useful help and Lonza group for supplying the Lonzacure Detda 80. The authors acknowledge the financial support of the French National Agency for Research (ANR) through the MAFESMA project. They also thank the European Science Foundation.

## Reference

- [1] G. B. Olson, M. Cohen, Metall. Trans. A **13A** 1907(1982)
- [2] T. Saburi, in: K. Otsuka, C.M. Wayman (Eds.), shape memory materials, Cambridge University Press, 1999, pp. 49-96.
- [3] S. Marfia, International Journal of Solids and Structures **42** 3677 (2005)
- [4] C.K. Poon, K.T. Lau, L.M. Zhou, Composites Part B: Engineering **36** 25 (2005)
- [5] S.Y. Fu, C.Y. Yue, X. Hu, Y.W. Mai, Composites Science and Technology **60** 569 (2000)
- [6] Y.C. Gao, L.M. Zhou, Energy Theoretical and Applied Fracture Mechanics **32** 203(1999)
- [7] C.Y. Yue, H.C. Looi, M.Y. Quek, Int J Adhesion and Adhesives **15** 73 (1995)
- [8] R.B. Yallee, R.J. Young, Composites Science and Technology **58** 1907(1998).
- [9] X.F. Zhou, J.A. Nairn, H.D. Wagner, Composites Part A **30** 1387(1999).
- [10] J.M. Vazquez-Rodriguez, P.J. Herrera-Franco, P.I. Gonzalez-Chi, Composites Part A **38** 819(2007)
- [11] M.Y. Quek, Int J of Adhesion & Adhesives **22** 303(2002)
- [12] D.J. Bannister, M.C. Andrews, A.J. Cervenka, R.J. Young, Composites Science and Technology **53** 411 (1995)
- [13] W. Beckert, B. Lauke, Composites science and technology **57** 1689 (1997)
- [14] Y.C. Gao, L.M. Zhou, Theoretical and Applied Fracture Mechanics **30** 235(1998)
- [15] X. Wang, G. Hu, Composites Part A **36** 1142 (2005).
- [16] C.K. Poon, L.M. Zhou, L.H. Yam, Composite Structures **66** 503 (2004).
- [17] K. Jonnalagadda, G.E. Kline, N.R. Sottos, Exp. Mech. **37** 78 (1997)
- [18] J.S.N. Paine, C.A. Rogers, in: Adaptive Structures and Material Systems, New York: ASME, AD **35** 63 (1993).
- [19] S. Rossi, F. Deflorian, A. Pegoretti, D. D'Orazio, S. Gialanella, Surface & Coatings Technology **202** 2214 (2008).
- [20] Y. Payandeh, F. Meraghni, E. Patoor, A. Eberhardt, Mater. Sci. Eng. A (2009); doi: 10.1016/j.msea.2009.04.019.